Physics of the Dark Universe 52 (2026) 102253

Contents lists available at ScienceDirect

Physics of the Dark Universe

journal homepage: www.elsevier.com/locate/dark

Gravitational lensing around quantum-corrected black holes within plasma environment

Bekzod Rahmatov [a,b,c,*], Isomiddin Nishonov [d], Sardor Murodov [e,f], Islom Egamberdiev [g], Otabek Umarov [h], Shavkat Karshiboev [i], Murodbek Vapayev [j], Muhammad Matyoqubov [k]

[a] University of Tashkent for Applied Sciences, Str. Gavhar 1, Tashkent, 100149, Uzbekistan
[b] Tashkent International University of Education, Imom Bukhoriy 6, Tashkent, 100207, Uzbekistan
[c] Tashkent State Technical University, Tashkent, 100095, Uzbekistan
[d] Ulugh Beg Astronomical Institute, Astronomy str. 33, Tashkent, 100052, Uzbekistan
[e] New Uzbekistan University, Movarounnahr Street 1, Tashkent, 100007, Uzbekistan
[f] Institute of Fundamental and Applied Research, National Research University TIIAME, Kori Niyoziy 39, Tashkent, 100000, Uzbekistan
[g] Samarkand State Architecture and Construction University named after Mirzo Ulugbek, Lolazor street 70, Samarqand, 140143, Uzbekistan
[h] Department of Exact Sciences, Kimyo International University in Tashkent, Shota Rustaveli Str. 156, Tashkent, 100121, Uzbekistan
[i] Samarqand State Pedagogical Institute, Spitamen Shokh Street 166, Samarkand, 140100, Uzbekistan
[j] Department of Technique, Urgench State University, Kh. Alimjan Str. 14, Urgench, 221100, Uzbekistan
[k] Mamun University Bolkhovuz Street 2, Khiva, 220900, Uzbekistan

ARTICLE INFO

Keywords:
Quantum-corrected black holes
KS black hole
Gravitational lensing
Black hole shadow
Plasma medium
Einstein ring

ABSTRACT

We explore the optical characteristics of the spacetime surrounding a quantum-corrected Kazakov–Solodukhin (KS) black hole, with particular attention to its shadow geometry, weak gravitational lensing behavior, and magnification effects. Our analysis shows that the quantum correction parameter of the KS metric plays a central role in determining these optical phenomena. An increase in this parameter leads to a larger photon sphere radius and, consequently, an expansion in the apparent size of the black hole shadow. Moreover, the presence of a plasma medium further enhances the shadow radius, with the plasma frequency exerting a noticeable influence on the observed image. In the weak-field regime, we find that both the bending angle of light and the corresponding magnification factors exhibit mild but systematic growth with increasing quantum correction parameter and plasma frequency. Based on these dependencies, we derive indicative observational constraints on the quantum correction parameter using measurable optical features of the system. Furthermore, by employing the gravitational lens equation, we investigate the magnification of the source brightness and determine the Einstein angle in a plasma environment .

1. Introduction

Black holes represent one of the most profound predictions of Einstein's general relativity (GR), serving as natural laboratories for probing gravity in its strongest regime [1,2]. Although GR has been rigorously tested in the weak-field limit through solar system experiments [3] and confirmed by the detection of gravitational waves [4,5], its validity in regions of extreme spacetime curvature near singularities remains uncertain. The inevitable breakdown of classical GR at singularities underscores the need for quantum gravity corrections, motivating the development of regular black hole models that eliminate curvature divergences while preserving the asymptotic behavior of GR [6].

Among the semiclassical approaches addressing this issue, the Kazakov–Solodukhin (KS) black hole [7] provides a particularly illuminating framework for exploring quantum gravitational effects. This quantum-corrected solution modifies the Schwarzschild metric by introducing a nonsingular core governed by a deformation parameter that encapsulates leading-order quantum corrections. Owing to its mathematical simplicity and clear physical motivation, the KS spacetime has attracted significant attention. Its physical properties have been extensively examined in various contexts, including shadow morphology [8,9], quasi-normal modes [9,10], accretion processes [11–13], gravitational lensing [14], and Hawking radiation [15,16]. Collectively, these studies demonstrate that the KS metric offers a promising theoret-

* Corresponding author.
E-mail addresses: rahmatovbekzod@samdu.uz (B. Rahmatov), s.murodov@newuu.uz (S. Murodov), egamberdiyev.islom@samdaqu.edu.uz (I. Egamberdiev), shavkat.qarshiboyev.89@bk.ru (S. Karshiboev), murodbek.v@urdu.uz (M. Vapayev), m_matyoqubov@mamunedu.uz (M. Matyoqubov).

https://doi.org/10.1016/j.dark.2026.102253
Received 27 November 2025; Received in revised form 5 February 2026; Accepted 16 February 2026
Available online 18 February 2026
2212-6864/© 2026 Elsevier B.V. All rights are reserved, including those for text and data mining, AI training, and similar technologies.

ical setting for investigating the observable manifestations of quantum gravity through astrophysical observations.

Gravitational lensing-one of the most striking predictions of GR-occurs when light from a distant source is deflected by the curvature of spacetime around a massive object [17]. The first observational confirmation of this phenomenon was made by Eddington during the 1919 solar eclipse [18], marking a milestone in the experimental verification of Einstein's theory. In the vicinity of black holes, where gravitational fields reach extreme intensities, lensing effects become particularly intriguing [19]. The study of weak gravitational lensing-where deflection angles are small and occur far from the event horizon-offers a valuable tool for understanding the nature of spacetime around compact objects and testing alternative theories of gravity. Furthermore, weak lensing has been instrumental in probing the large-scale structure of the Universe, constraining dark matter and dark energy models [20–23].

Theoretical investigations of weak lensing by different black hole geometries have revealed how spacetime curvature and additional parameters affect light trajectories [24–26]. For instance, Virbhadra and Ellis [27] provided a detailed analysis of weak lensing in Schwarzschild spacetime, while subsequent works extended the analysis to rotating Kerr black holes [28]. Numerous studies have further explored lensing in more generalized or modified spacetimes [29–49]. These analyses confirm that gravitational lensing serves as a precise diagnostic tool for testing the predictions of GR and its quantum-corrected extensions.

In realistic astrophysical environments, black holes are often surrounded by plasma, originating from accretion disks or interstellar material. The interplay between gravitational and plasma effects introduces additional complexity into the propagation of light [50–52]. Plasma modifies the effective refractive index of the medium, thereby altering observable quantities such as deflection angles, magnification factors, and the apparent shadow size [53–72]. In particular, the presence of plasma has been shown to modify the shadow structure of black holes [73–87].

With the advent of high-resolution interferometric observations-most notably, the Event Horizon Telescope (EHT) images of M87* and Sgr A* [88,88–94]-the study of plasma effects and quantum corrections in gravitational lensing has gained new significance. Plasma-induced modifications to shadow morphology and lensing observables can serve as potential signatures of new physics beyond classical GR.

In this work, we investigate the optical properties of the Kazakov–Solodukhin (KS) black hole under the influence of a surrounding plasma medium. Specifically, we analyze weak gravitational lensing, shadow morphology, and magnification effects, emphasizing how the quantum correction parameter and plasma frequency jointly affect these observables. We also employ the gravitational lens equation to determine image magnification and the Einstein angle. Our results provide new insights into how quantum-gravity-induced corrections and plasma environments modify the observational appearance of black holes.

The structure of this paper is as follows. In Section 2, we discuss photon motion around the KS black hole in a plasma medium using the Hamilton–Jacobi formalism. In Section 3, we analyze weak gravitational lensing and derive the deflection angle. In Section 4, we compute image magnification using the lens equation. Finally, Section 5 summarizes our main results and implications. Throughout this paper, we adopt geometric units with ($c = 1$ and $G = 1$).

2. Dynamics around black hole

2.1. Kazakov–Solodukhin (KS) black hole

The Kazakov–Solodukhin (KS) black hole represents a quantum-gravity inspired deformation of the Schwarzschild geometry that incorporates leading-order quantum corrections derived from the renormalization group approach [7]. This model arises from considering spherically symmetric quantum fluctuations of the spacetime metric within an effective two-dimensional dilaton gravity framework. Through this formulation, one can consistently regularize the curvature singularity at the origin while maintaining the classical asymptotic flatness at spatial infinity. In this sense, the KS metric provides a phenomenologically viable model that bridges classical general relativity and quantum gravity corrections.

The static and spherically symmetric KS spacetime is described by the line element

$$ds^2 = -f(r)dt^2 + f(r)^{-1}dr^2 + r^2(d\theta^2 + \sin^2\theta\, d\phi^2), \tag{1}$$

where the lapse function $f(r)$ is determined through an integral relation involving an effective renormalizable potential $U(\rho)$,

$$f(r) = -\frac{2M}{r} + \frac{1}{r}\int^r U(\rho)\, d\rho. \tag{2}$$

The potential $U(\rho)$ characterizes the transition between the classical and quantum domains, taking the following form:

$$U(\rho, t) = \begin{cases} 0, & 0 \le \rho \le 4\sqrt{\kappa t}, \\ \dfrac{\rho}{\sqrt{\rho^2 - 16\kappa t}}, & \rho > 4\sqrt{\kappa t}, \end{cases} \tag{3}$$

where the renormalization scale parameter $t = \ln(\mu/\mu_0)$ encodes the quantum corrections through the running of the gravitational coupling constant. After integrating Eq. (2), the metric function can be expressed in a compact analytical form as

$$f(r) = \frac{\sqrt{r^2 - \beta^2}}{r} - \frac{2M}{r}. \tag{4}$$

Here, $\beta^2 = 4G_R/\pi$ is a renormalization group-induced scale that quantifies the departure from classical general relativity. It originates from integrating out short-distance metric fluctuations, leading to a renormalization of Newton's constant: $G_R = G_N \ln(\mu/\mu_0)$. Physically, this parameter can be interpreted as a minimal length scale (or "quantum hair") inherent to the black hole, connected to Planck-scale physics. It regulates the central singularity, replacing it with a smooth, non-singular core of size $\sim \beta$. In our phenomenological analysis, we explore a possible broader range of β values to illustrate the qualitative effects of the deformation, as $0 < |\beta| < 0$. While, the minimal value of it supposed to be equal to the Planck radius $r_{pl} = \sqrt{\hbar G_N/c^3}$ by assuming that possible factors ~ 10 are non-essential. In the limit $\beta \to 0$, these quantum corrections vanish, and the standard Schwarzschild solution of general relativity is smoothly recovered.

Physically, the presence of β modifies the near-horizon structure and photon dynamics around the black hole, leading to measurable effects on observable quantities such as the shadow radius, lensing deflection angle, and emission profiles. Hence, the KS black hole serves as an important theoretical model for exploring potential signatures of quantum gravity in astrophysical observations.

2.2. Null geodesics around the KS black hole in plasma

In this subsection, we examine the propagation of photons in the vicinity of a Kazakov–Solodukhin (KS) black hole when the surrounding environment contains a non-magnetized, pressureless plasma. The presence of plasma modifies the trajectories of light rays due to the frequency-dependent refractive index of the medium, leading to important observational consequences for black hole shadow and lensing phenomena.

To describe photon motion in such a medium, it is convenient to employ the Hamilton–Jacobi formalism. The Hamiltonian of a photon propagating in plasma can be expressed as Synge [95]

$$H(x^\alpha, p_\alpha) = \frac{1}{2}\tilde{g}^{\alpha\beta}p_\alpha p_\beta, \tag{5}$$

where x^α denotes the spacetime coordinates, and $\tilde{g}^{\alpha\beta}$ represents the effective optical metric tensor in the presence of plasma. The latter is defined by

$$\tilde{g}^{\alpha\beta} = g^{\alpha\beta} - (n^2 - 1)u^\alpha u^\beta, \tag{6}$$

where u^α is the four-velocity of the observer measuring the photon frequency, and n is the refractive index of the plasma medium. The refractive index can be expressed as Bisnovatyi-Kogan and Tsupko [52]

$$n^2 = 1 - \frac{4\pi e^2 N(r)}{m_e \omega(r)^2}, \tag{7}$$

where e and m_e are the charge and mass of the electron, respectively, and $N(r)$ is the local number density of electrons. The photon frequency $\omega(r)$ as measured by a static observer at radius r is redshifted due to the gravitational field, and it can be written as Bisnovatyi-Kogan and Tsupko [52]

$$\omega(r) = \frac{\omega_0}{\sqrt{f(r)}}, \tag{8}$$

where ω_0 is the photon frequency measured by a distant observer at infinity. The propagation of light through plasma is only possible when $\omega(r) > \omega_p(r)$, which ensures that the refractive index $n > 0$.

The circular photon orbits define the photon sphere of the black hole, whose radius $r_{\rm ph}$ can be found by imposing the extremum condition on the impact parameter. This condition is expressed as Perlick et al. [96]

$$\frac{d(h^2(r))}{dr}\Big|_{r=r_{\rm ph}} = 0, \tag{9}$$

where

$$h^2(r) \equiv r^2 \left[\frac{1}{f(r)} - \frac{\omega_p^2(r)}{\omega_0^2}\right]. \tag{10}$$

By combining Eqs. (9) and (10), one obtains an algebraic equation that determines the radius of the photon sphere in the presence of a plasma medium:

$$1 - \frac{2M^2(\beta^2 + 8M^2 - 2Mr_{\rm ph})}{(-\beta^2 - 8M^2 + 4Mr_{\rm ph})^2} = \frac{\omega_p^2(r_{\rm ph})}{\omega_0^2} + \frac{r_{\rm ph}\omega_p(r_{\rm ph})\omega'(r_{\rm ph})}{\omega_0^2}. \tag{11}$$

Here, the prime denotes differentiation with respect to the radial coordinate r. In general, this equation cannot be solved analytically for arbitrary plasma distributions. This can be solved only for uniform plasma distribution and in the case of $\beta = 0$, which can then be written:

$$r_{ph} = \frac{-4\frac{\omega_p^2}{\omega_0^2} + \sqrt{9 - 8\frac{\omega_p^2}{\omega_0^2}} + 3}{2 - 2\frac{\omega_p^2}{\omega_0^2}}.$$

We can easily see that this solution will reproduce photon sphere radius in schwarzschild spacetime in vacuum case, if we plug $\omega_p^2/\omega_0^2 = 0$. To include effects of quantum correction parameter β, we choose following plasma distributions, and we will do numerical analysis during these two subsections.

2.3. Homogeneous plasma

The most commonly used "toy models" for plasma distribution are homogeneous plasma [65,97–101], therefore we first analyze the case of a homogeneous (uniform) plasma, where the plasma frequency is spatially constant, i.e., $\omega_p^2(r) = \text{const}$. Although Eq. (11) cannot be solved analytically even in this case, the dependence of the photon sphere radius $r_{\rm ph}$ on the model parameters can be explored graphically. As illustrated in Fig. 1 (upper panel), the radius of the photon sphere increases with both the quantum correction parameter β/M and the plasma frequency ω_p. This implies that the effect of quantum corrections tends to enlarge the apparent shadow size of the KS black hole, while plasma negatively affects.

2.4. Inhomogeneous plasma

The environment around Supermassive black holes is characterized by a radiatively inefficient accretion flow (RIAF), such as an advection-dominated accretion flow (ADAF). The electron density in such flows is well-described by a power-law profile from the Bondi radius inwards. Observational constraints from stellar orbits, Faraday rotation, and sub-mm imaging suggest a density profile with $k \sim 1-2$ on the relevant scales ($\sim 10^2 - 10^5$ gravitational radii) [61,97–101]. Therefore, the power-law plasma model is the most physically realistic for especially Sgr A* which we planned eventually constraint our parameters from EHT observations. Next, we consider an inhomogeneous plasma distribution characterized by a simple power-law profile [53]:

$$\omega_p^2(r) = \frac{z_0}{r^q}, \tag{12}$$

where z_0 and $q > 0$ are free parameters controlling the plasma density and its radial falloff, respectively. To capture the essential behavior of such a medium, we restrict our analysis to the representative cases $q = 1$ and $q = 2$. Using Eqs. (11) and (12), the photon sphere radius $r_{\rm ph}$ can be evaluated numerically for different parameter values.

From Fig. 1 (middle and lower panels), it is evident that in the case of an inhomogeneous plasma with $q = 1$, the photon sphere radius increases with both β/M and the ratio $z_0/(M\omega_0^2)$. Interestingly, for the case $q = 2$, corresponding to a singular isothermal sphere distribution, the photon sphere radius becomes independent of the plasma frequency. This behavior indicates that the plasma influence on photon motion strongly depends on the density profile, revealing how different astrophysical plasma environments can alter the observable shadow structure of quantum-corrected black holes.

2.5. Black hole shadow in a plasma environment with different distributions

In this subsection, we investigate the influence of plasma on the apparent shadow of the Kazakov–Solodukhin (KS) black hole. The presence of plasma modifies the trajectories of photons due to refraction, which in turn alters the perceived size and shape of the black hole shadow. This effect becomes particularly relevant in realistic astrophysical settings, where accretion flows and surrounding plasma can significantly impact observational features detected by very long baseline interferometry (VLBI) experiments.

The angular radius of the black hole shadow, denoted by $\alpha_{\rm sh}$, can be derived geometrically from the photon motion in the plasma medium. Following Refs. [79,96,102,103], it is expressed as

$$\sin^2 \alpha_{\rm sh} = \frac{h^2(r_p)}{h^2(r_0)}, \tag{13}$$

where r_p represents the photon sphere radius and r_0 is the radial position of the observer.

For an observer located at a large distance from the black hole ($r_0 \to \infty$), the apparent radius of the shadow can be approximated as Perlick et al. [96], Raza et al. [104]

$$R_{\rm sh} \approx r_0 \sin\alpha_{\rm sh} = \sqrt{r_p^2\left[\frac{1}{f(r_p)} - \frac{\omega_p^2(r_p)}{\omega_0^2}\right]}, \tag{14}$$

where $f(r)$ is the metric function and $\omega_p(r)$ denotes the plasma frequency. This approximation follows from the asymptotic behavior $h(r) \to r$ at spatial infinity, which holds for all plasma models considered.

For a black hole immersed in a uniform plasma, the shadow radius $R_{\rm sh}$ can be determined numerically. Fig. 2 presents the numerical results for different plasma configurations as a function of the spacetime parameter β/M. It can be observed that the quantum correction parameter β has a positive influence on the shadow size regardless of the plasma distribution. In contrast, increasing the plasma frequency generally leads to a decrease in the shadow radius for all considered models ($q = 0, 1, 2$). This behavior can be attributed to the refractive index of the plasma, which causes photons with lower frequencies to bend more strongly, effectively reducing the observed angular size of the shadow.

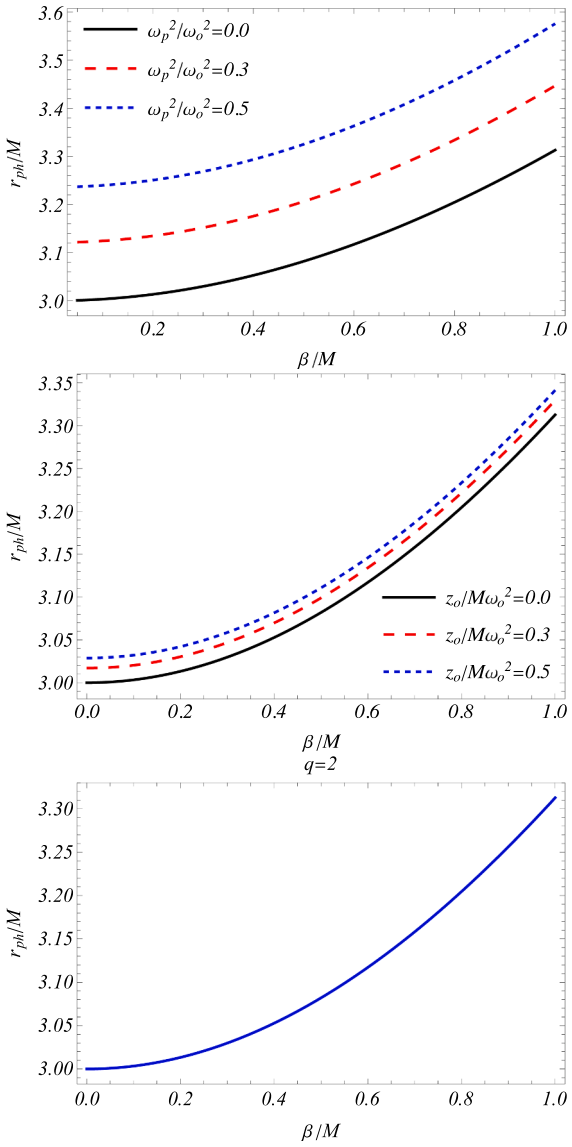

Fig. 1. The dependence of the photon sphere radius on the effective charge for various frequency values in homogeneous (upper panel) and inhomogeneous plasmas with $q = 1$ (middle panel) and the singular isothermal sphere (SIS) case with $q = 2$ (lower panel).

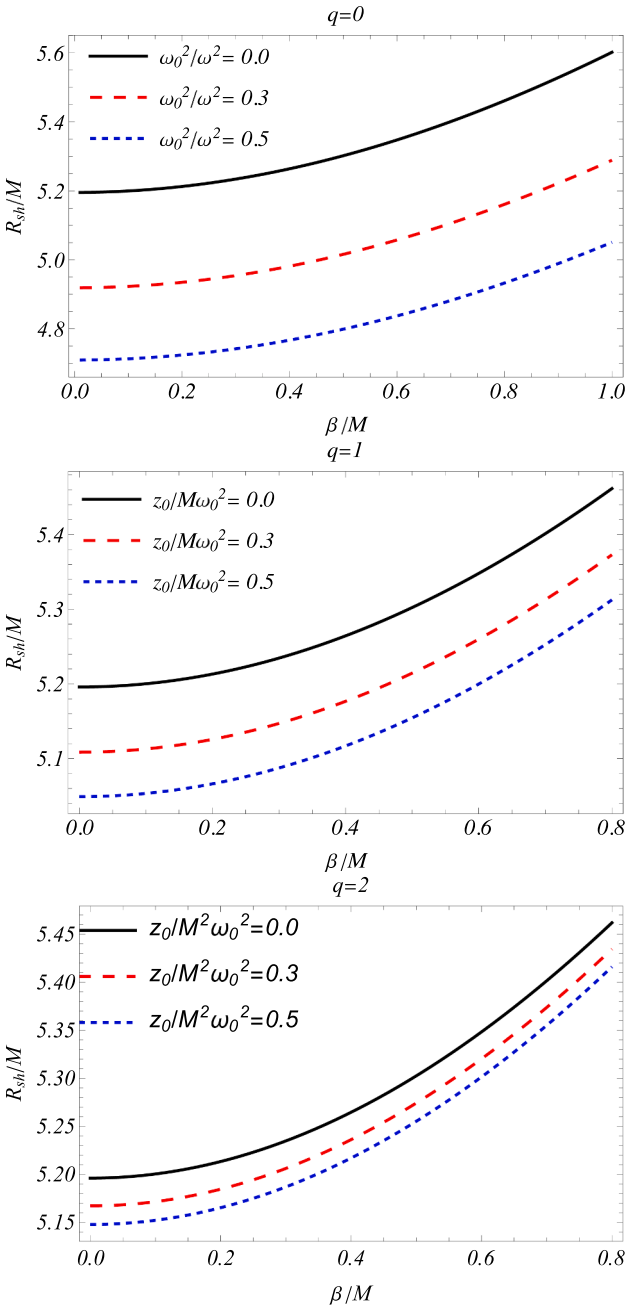

Fig. 2. Variation of the black hole shadow radius with the quantum correction parameter β/M for different plasma frequency values in homogeneous (upper panel) and inhomogeneous ($q = 1$, $q = 2$; middle and lower panels) plasma distributions.

Thanks to the recent high-resolution observations of the Event Horizon Telescope (EHT) Collaboration [105,106], it has become possible to place empirical constraints on the parameters of modified gravity models and their surrounding plasma environments. The observed shadow diameter of Sgr A* provides bounds on the dimensionless shadow radius as $4.55 \leq R_{\rm sh}/M \leq 5.22$ and $4.21 \leq R_{\rm sh}/M \leq 5.56$, corresponding to the 1σ and 2σ confidence intervals, respectively [107].

The constraints illustrated in Fig. 3 show that the allowed range of the quantum correction parameter β/M is highly sensitive to the plasma frequency. For instance, within 1σ, the parameter β/M lies between 0 and 0.3 for $\omega_0^2/\omega^2 = 0$, whereas this range can extend up to $\beta/M \approx 1$ for $\omega_0^2/\omega^2 = 0.5$. More generally, within the 2σ uncertainty range, β/M may take any value consistent with the physical constraint that prevents the emergence of a naked singularity. We emphasize that these constraints are derived under the assumption of a fixed plasma profile and do not incorporate systematic uncertainties associated with accretion flow modeling, plasma distribution, or observational calibration. Consequently, the inferred bounds on β/M should be interpreted as indicative constraints that reflect the sensitivity of shadow observables to quantum corrections, rather than as definitive parameter limits.

Interestingly, for the singular isothermal sphere ($q = 2$) plasma distribution, the constraints exhibit a weaker dependence on the plasma frequency. As shown in the lower panel of Fig. 3, it becomes difficult to distinguish between plasma and vacuum environments observationally. This result suggests that shadow-based constraints alone may not suffice to determine the precise plasma configuration surrounding the black hole, emphasizing the need for complementary probes such as polarization and lensing observations to fully characterize quantum-corrected black holes. Finally, we present a quantitative comparison of the Kazakov–Solodukhin (KS) black hole with the standard Schwarzschild spacetime and a representative regular black hole

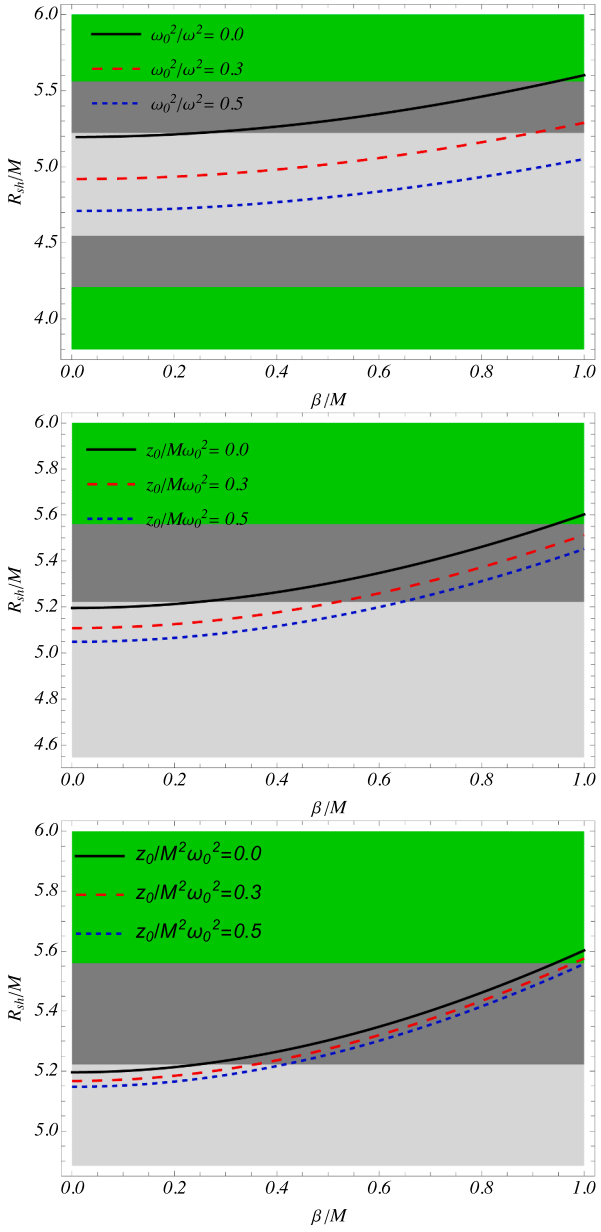

Fig. 3. Constraints on the quantum-correction parameter β/M and the plasma parameter ω_0^2/ω^2 based on EHT observations of Sgr A* for different plasma distributions.

model, namely the Bardeen black hole[6], as shown in Fig. 4. The figure displays the corresponding photon sphere radius and shadow radius for all three geometries, evaluated for the same black hole mass and plasma configuration. From Fig. 4, it is evident that while all models coincide with the Schwarzschild limit for vanishing deformation parameters, the KS black hole exhibits systematic and increasingly pronounced deviations in both the photon sphere and shadow radius as the quantum correction parameter β/M, l_0/M increases. These deviations are qualitatively and quantitatively distinct from those arising in the Bardeen spacetime, where modifications are controlled by the nonlinear electrodynamics deformation parameter. In particular, for comparable deformation strengths, the KS black hole leads to a larger photon sphere and shadow radius than the Bardeen model, indicating that the underlying quantum correction mechanism produces observationally distinguishable signatures.

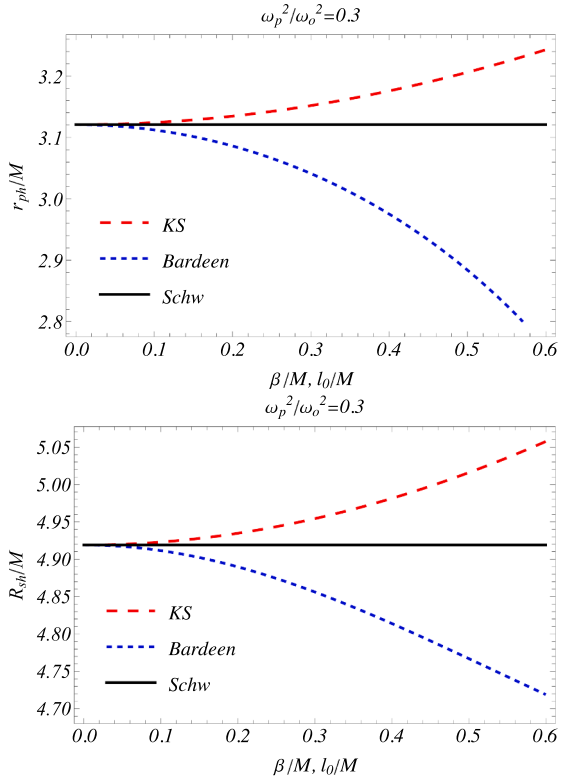

Fig. 4. Difference between predicts of three different black hole spacetimes, KS, Schwarzschild and Bardeen, for photon sphere and shadow radius.

3. Gravitational weak lensing in plasma medium

In this section, we analyze the influence of plasma surrounding a black hole on the propagation of light rays. We assume that light rays with impact parameters $b >> r_{ph}$, where r_{ph} denotes the photon sphere radius of the Kazakov–Solodukhin black hole. In this regime, the gravitational field along the photon trajectory remains weak, and the deflection angle can be consistently expanded to leading order in $M/b, \beta/b$. Typical impact parameters are of astrophysical scale (kiloparsecs), while the gravitational radius $\sim M$ and the quantum-correction scale β remain many orders of magnitude smaller. Consequently, quantum corrections enter as small perturbative contributions to the classical Schwarzschild deflection angle and do not invalidate the weak-field expansion. The theoretical framework follows the formalism developed by Synge [95], which accounts for the dispersive properties of plasma in curved spacetime. The weak gravitational field approximation allows us to express the spacetime metric as a small perturbation of the flat Minkowski background [52]:

$$g_{\alpha\beta} = \eta_{\alpha\beta} + h_{\alpha\beta}, \tag{15}$$

where $\eta_{\alpha\beta}$ and $h_{\alpha\beta}$ denote the Minkowski metric and a small perturbation, respectively. These quantities satisfy

$$\begin{aligned} &\eta_{\alpha\beta} = \mathrm{diag}(-1,1,1,1), \\ &h_{\alpha\beta} \ll 1, \quad h_{\alpha\beta} \to 0 \quad \text{as} \quad x^\alpha \to \infty, \\ &g^{\alpha\beta} = \eta^{\alpha\beta} - h^{\alpha\beta}, \quad h^{\alpha\beta} = h_{\alpha\beta}. \end{aligned} \tag{16}$$

The phase velocity of electromagnetic waves in a plasma is determined by $v = c/n$, where n is the refractive index. From Eq. (7), it follows that when $\omega_p > \omega$, the plasma behaves as a *refractive* medium, in which electromagnetic waves cannot propagate due to the high density of free electrons. Conversely, when $\omega_p < \omega$, the plasma acts as a *dispersive* or reflective medium, allowing partial propagation. In the limit $\omega_p \ll \omega$, we recover $n \to 1$, corresponding to the vacuum case.

To quantify the influence of plasma on gravitational light deflection, the deflection angle in the presence of plasma can be expressed as Bisnovatyi-Kogan and Tsupko [52], Atamurotov et al. [79]

$$\hat{\alpha}_i = \frac{1}{2}\int_{-\infty}^{\infty}\left(h_{33} + \frac{h_{00}\omega^2 - K_e N(x^i)}{\omega^2 - \omega_e^2}\right)_{,i} dz, \tag{17}$$

where i represents the one of the coordinate (we can later choose it as b which is related to radial distance by $b^2 = r^2 - z^2$).

A negative value of $\hat{\alpha}_b$ corresponds to the deflection of light rays toward the central compact object, while positive values correspond to deflection away from it. For sufficiently large r, such that $\frac{R_s}{r} \gg (\frac{R_s}{r})^2$, the black hole metric can be approximated by

$$ds^2 = ds_0^2 + \left(\frac{R_s}{r} + \frac{\beta^2}{2r^2}\right)dt^2 + \left(\frac{R_s}{r} + \frac{\beta^2}{2r^2}\right)dr^2, \tag{18}$$

where $ds_0^2 = -dt^2 + dr^2 + r^2(d\theta^2 + \sin^2\theta\, d\phi^2)$ is the flat spacetime line element.

We now investigate the combined effects of the plasma medium and the gravitational field of the Sen black hole, using the above formalism. In Cartesian coordinates, the metric perturbations $h_{\alpha\beta}$ can be written as

$$\begin{aligned} h_{00} &= \frac{R_s}{r} + \frac{\beta^2}{2r^2}, \\ h_{ik} &= \left(\frac{R_s}{r} + \frac{\beta^2}{2r^2}\right)n_i n_k, \\ h_{33} &= \left(\frac{R_s}{r} + \frac{\beta^2}{2r^2}\right)\cos^2 x, \end{aligned} \tag{19}$$

where $R_s = 2M$, $\cos x = z/\sqrt{b^2+z^2}$, and $r = \sqrt{b^2+z^2}$. The quantity b denotes the impact parameter, representing the closest approach of the light ray to the black hole.

Using the above mentioned expressions in the formula, one can compute the light deflection angle with respect to b for a black hole surrounded by plasma

$$\hat{\alpha}_b = \int_{-\infty}^{\infty}\frac{1}{2}\left[\partial_b dh_{33} + \right. \\ \left. + \frac{\omega^2}{\omega^2 - \omega_e^2}\partial_b h_{00} - \frac{K_e}{\omega^2 - \omega_e^2}\partial_b N(r)\right]dz. \tag{20}$$

or with the relationship, $\partial_b = \frac{b}{r}\partial_r$, we can rewrite this as follows

$$\hat{\alpha}_b = \int_{-\infty}^{\infty}\frac{b}{2r}\left[\frac{dh_{33}}{dr} + \right. \\ \left. + \frac{dh_{00}}{dr}\frac{\omega^2}{\omega^2 - \omega_e^2} - \frac{K_e}{\omega^2 - \omega_e^2}\frac{dN(r)}{dr}\right]dz. \tag{21}$$

From Eq. (21), one can see that the total deflection angle incorporates both gravitational and plasma effects. To better understand their individual contributions, it is convenient to decompose the total deflection angle into three separate integrals that account for different physical influences [56]:

$$\hat{\alpha}_1 = \frac{1}{2}\int_{-\infty}^{\infty}\frac{b}{r}\left(\frac{dh_{33}}{dr}\right)dz, \tag{22}$$

$$\hat{\alpha}_2 = \frac{1}{2}\int_{-\infty}^{\infty}\frac{b}{r}\left(\frac{1}{1-\omega_e^2/\omega^2}\frac{dh_{00}}{dr}\right)dz, \tag{23}$$

$$\hat{\alpha}_3 = -\frac{1}{2}\int_{-\infty}^{\infty}\frac{b}{r}\left(\frac{K_e}{\omega^2 - \omega_e^2}\frac{dN(r)}{dr}\right)dz. \tag{24}$$

These terms correspond, respectively, to (i) the pure spacetime curvature contribution, (ii) the mixed contribution from both gravity and plasma, and (iii) the correction arising solely from the spatial variation of plasma density.

In what follows, we compute the integrals for different plasma configurations and analyze how each distribution modifies the deflection behavior of photons near the black hole.

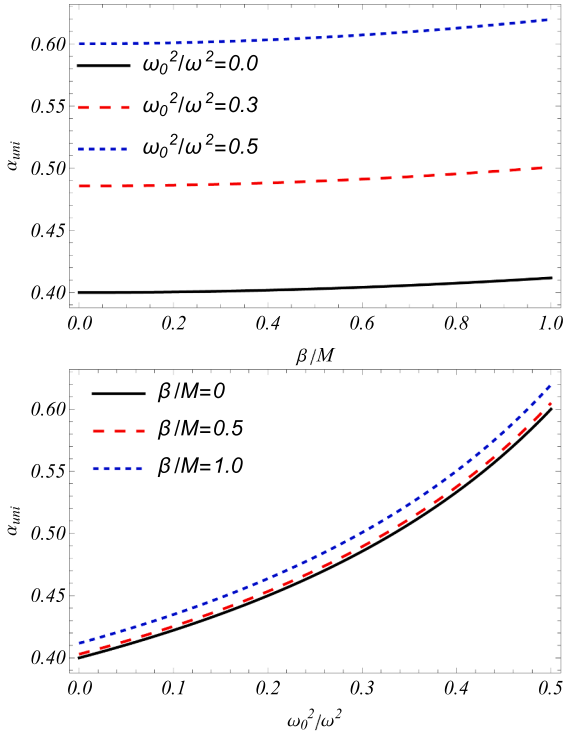

Fig. 5. Dependence of the deflection angle of light rays in the presence of a uniform plasma on the impact parameter b for different values of the quantum parameter β (upper panel) and plasma frequency (lower panel).

3.1. Uniform plasma

We begin with the simplest case of a uniform plasma distribution as we did in the shadow part. For this configuration, the first term in Eq. (22)-which represents the contribution due solely to spacetime curvature-takes the form:

$$\hat{\alpha}_1 = \frac{1}{2}\int_{-\infty}^{\infty}\frac{b}{r}\left(\frac{dh_{33}}{dr}\right)dz = -\frac{R_s}{b} - \frac{\pi\beta^2}{8b^2}. \tag{25}$$

From Eq. (25), one observes that in the limit $\beta = 0$ the deflection angle reduces to the Schwarzschild case $\hat{\alpha}_1 = -R_s/b$. The second term, which mixes the effects of gravity and plasma, can be written as:

$$\hat{\alpha}_2 = \frac{1}{2}\int_{-\infty}^{\infty}\frac{b}{r}\left(\frac{1}{1-\omega_e^2/\omega^2}\frac{dh_{00}}{dr}\right)dz = -\frac{R_s}{b(1-\omega_0^2/\omega^2)} - \\ - \frac{\pi\beta^2}{4b^2(1-\omega_0^2/\omega^2)}, \tag{26}$$

where $\omega_0^2 = \omega_e^2 = \text{const}$. In the limit $\beta \to 0$, Eq. (26) reduces to $\hat{\alpha}_2 = -R_s/b$. Hence, for $\beta = 0$, the total deflection angle recovers the classical Schwarzschild result $\hat{\alpha}_b = 2R_s/b$.

In the case of a uniform plasma, the third contribution in Eq. (24) vanishes, since the plasma density is spatially constant and $\partial_r N(r) = 0$. Therefore, the total deflection angle can be expressed as

$$\hat{\alpha}_{\text{uni}} = \left(1 + \frac{1}{1-\frac{\omega_0^2}{\omega^2}}\right)\frac{R_s}{b} + \left(1 + \frac{2}{1-\frac{\omega_0^2}{\omega^2}}\right)\frac{\pi\beta^2}{8b^2}. \tag{27}$$

Fig. 5 illustrates the dependence of the photon deflection angle $\hat{\alpha}_{\text{uni}}$ on both the quantum correction parameter β/M and the plasma parameter ω_0^2/ω^2. As seen, increasing β leads to a slight enhancement in the deflection angle, while a denser plasma (higher ω_0^2/ω^2) further increases the deflection. Consequently, the bending of light in a uniform plasma environment is stronger than in the vacuum case.

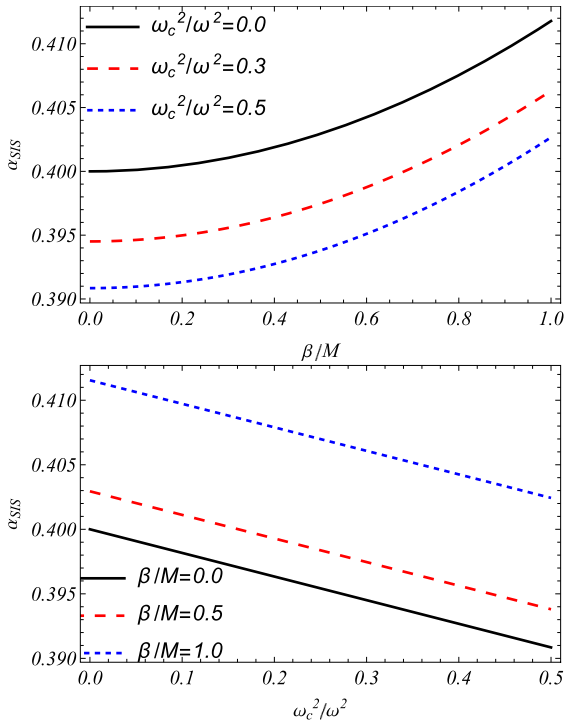

Fig. 6. Dependence of the deflection angle of light rays in the presence of a non-uniform (SIS-type) plasma distribution on the impact parameter b for different values of β (upper panel) and plasma frequency ratio ω_c^2/ω^2 (lower panel).

3.2. Singular isothermal sphere plasma

Next, we examine the case of a non-uniform plasma distribution following the Singular Isothermal Sphere (SIS) model, which provides a physically realistic description of galaxy or cluster-scale plasmas. The SIS represents a spherically symmetric distribution of ionized gas whose density decreases with radius according to Bisnovatyi-Kogan and Tsupko [52], Rogers [53]:

$$\rho(r) = \frac{\sigma_v^2}{2\pi r^2}, \tag{28}$$

where σ_v denotes the one-dimensional velocity dispersion. The corresponding plasma concentration can be written as Bisnovatyi-Kogan and Tsupko [52], Rogers [53]:

$$N(r) = \frac{\rho(r)}{km_p}, \tag{29}$$

where m_p is the proton mass and k is a dimensionless proportionality constant related to the effective mass-to-charge ratio of the plasma. The associated plasma frequency thus takes the form:

$$\omega_e^2 = K_e N(r) = \frac{K_e \sigma_v^2}{2\pi k m_p r^2}. \tag{30}$$

Using this distribution, one can compute the deflection angle in the presence of SIS-type plasma surrounding the Sen black hole by substituting into Eqs. (22)–(24). Following Atamurotov et al. [59], we express the total angle as

$$\hat{\alpha}_{\rm SIS} = \hat{\alpha}^{(1)}_{\rm SIS} + \hat{\alpha}^{(2)}_{\rm SIS} + \hat{\alpha}^{(3)}_{\rm SIS}, \tag{31}$$

where the first term, independent of plasma effects, coincides with Eq. (25). The remaining terms are given by:

$$\begin{aligned}\hat{\alpha}^{(2)}_{\rm SIS} &= \frac{1}{2}\int_{-\infty}^{\infty} \frac{b}{r}\left(\frac{1}{1-\omega_e^2/\omega^2}\frac{dh_{00}}{dr}\right)dz \\ &= -\frac{R_s}{b} + \frac{3\beta^2 R_s^2}{16b^4}\frac{\omega_c^2}{\omega^2} - \frac{2R_s^3}{3b^3\pi}\frac{\omega_c^2}{\omega^2} + \frac{\pi\beta^2}{4b^2},\end{aligned} \tag{32}$$

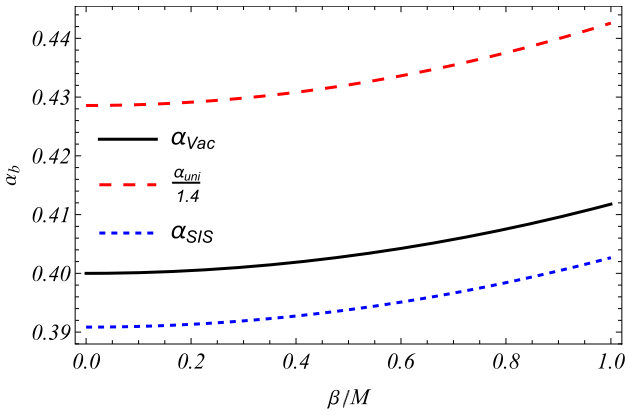

Fig. 7. Comparison of the deflection angle $\hat{\alpha}_b$ in three environments: vacuum, uniform plasma, and SIS plasma, as a function of the quantum-corrected parameter β. For better visualization, the uniform case $\hat{\alpha}_{\rm uni}$ is divided by 1.4.

$$\hat{\alpha}^{(3)}_{\rm SIS} \simeq -\frac{1}{2}\frac{K_e}{\omega^2}\int_{-\infty}^{\infty}\frac{b}{r}\frac{dN}{dr}dz = \frac{R_s^2}{2b^2}\frac{\omega_c^2}{\omega^2}, \tag{33}$$

where

$$\omega_c^2 = \frac{K_e\sigma_v^2}{2km_pR_s^2}. \tag{34}$$

Collecting all terms, the total deflection angle in the SIS plasma case becomes:

$$\hat{\alpha}_{\rm SIS} = \frac{2R_s}{b} + \frac{3\pi\beta^2}{8b^2} - \frac{\omega_c^2}{\omega^2}\frac{R_s^2}{b^2}\left(\frac{1}{2} - \frac{3\beta^2}{16b^2} - \frac{2R_s}{3b\pi}\right). \tag{35}$$

Fig. 6 depicts the variation of $\hat{\alpha}_{\rm SIS}$ as a function of β for different plasma parameters. The results show that both the uniform and SIS plasmas share similar qualitative behavior with respect to β, where increasing the quantum correction parameter tends to increase the deflection slightly. However, plasma inhomogeneity has the opposite effect-reducing the overall deflection magnitude compared to the uniform case. This reduction becomes more significant as ω_c^2/ω^2 increases, consistent with earlier studies [53,108].

Thus, the presence of SIS-type plasma around the black hole produces a notable impact on the trajectories of photons, reducing the bending angle relative to both the vacuum and uniform plasma cases. The comparative results for different plasma distributions are illustrated in Fig. 7.

4. Impact of plasma environment on Einstein angle and magnification

In this section, we investigate the observable consequences of gravitational lensing in the presence of a plasma medium, focusing particularly on the Einstein angle and the magnification of image brightness. These quantities depend directly on the deflection angle $\hat{\alpha}$ derived in the previous sections, especially for the case of uniform plasma. Fig. 9 schematically illustrates the gravitational lensing configuration, showing the alignment between the source, lens (black hole), and observer.

The basic lens equation relates the angular positions of the source γ and image θ, the deflection angle $\hat{\alpha}$, and the distances between the observer, lens, and source as

$$\theta D_s = \gamma D_s + D_{ls}\hat{\alpha}, \tag{36}$$

where D_s is the distance between the observer and source, and D_{ls} is the distance between the lens and the source. In the weak-field approximation, the impact parameter b can be expressed as $b \approx D_d\theta$, with D_d being the distance from the observer to the lens. Using this relation, Eq. (36) can be rewritten as

$$\gamma = \theta - \frac{D_{ds}}{D_s}\hat{\alpha}. \tag{37}$$

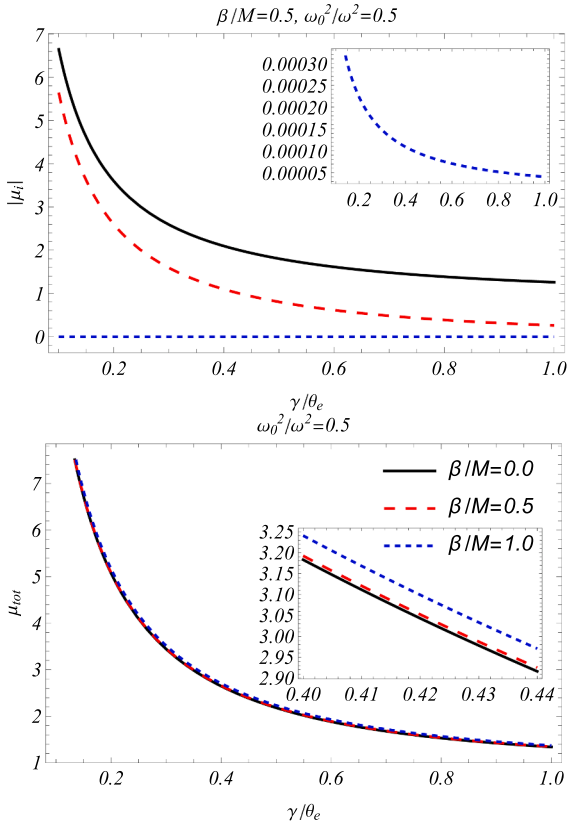

Fig. 8. (Upper panel) Magnification of images as a function of source position γ for $\omega_0^2/\omega^2 = 0.5$ and $\beta/M = 0.5$. The black solid, red dashed, and blue dotted curves represent the first, second, and tertiary weak-field images, respectively. (Lower panel) Total magnification of the source image as a function of γ for $\omega_0^2/\omega^2 = 0.5$ and various β values.(For interpretation of the references to colour in this figure legend, the reader is referred to the web version of this article.)

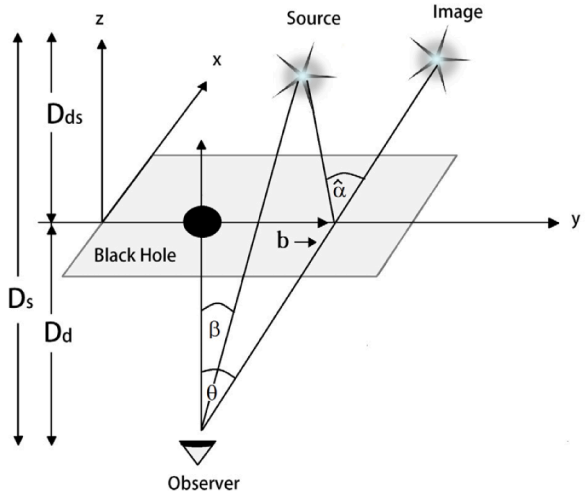

Fig. 9. Schematic view of the gravitational lensing system. The observer (O), lens (L), and source (S) are aligned along the optical axis, while the light from the source is deflected by the gravitational field of the lens.

Substituting the expression for $\hat{\alpha}$ in a uniform plasma (Eq. (27)) into Eq. (37), we obtain

$$\gamma = \theta - \frac{D_{ds}}{D_s D_d}\left(1 + \frac{1}{1-\frac{\omega_0^2}{\omega^2}}\right)\frac{R_s}{\theta} - \frac{\pi\beta^2}{8\theta^2}\left(1 + \frac{2}{1-\frac{\omega_0^2}{\omega^2}}\right)\frac{D_{ds}}{D_s D_d^2}. \tag{38}$$

To simplify the analysis, we introduce a new variable $x = \theta - \frac{\gamma}{3}$, reducing Eq. (38) to a cubic equation of the form

$$x^3 + px + l = 0, \tag{39}$$

where

$$p = -\frac{1}{3}\gamma^2 - \frac{1}{2}\left(1 - \frac{1}{\frac{\omega_0^2}{\omega^2} - 1}\right)\theta_E^2, \tag{40}$$

$$l = \left(1 - \frac{2}{\frac{\omega_0^2}{\omega^2} - 1}\right)\frac{\pi\beta^2\theta_E^2}{16 D_d R_s} - \left(1 - \frac{1}{\frac{\omega_0^2}{\omega^2} - 1}\right)\frac{\gamma\theta_E^2}{6} - \frac{2\gamma^3}{27}, \tag{41}$$

$$\theta_E = \sqrt{\frac{2R_s D_{ds}}{D_s D_d}}, \tag{42}$$

with θ_E denoting the Einstein ring angle.

The cubic Eq. (39) admits the general analytical solution [67,109]

$$x = 2s^{1/3}\cos\left(\frac{\phi + 2\pi k}{3}\right), \qquad k = 0, 1, 2, \tag{43}$$

where

$$s = \sqrt{-\frac{p^3}{27}}, \quad \phi = \arccos\left(-\frac{l}{2s}\right). \tag{44}$$

Each value of k corresponds to a distinct weak-field image position resulting from the modified lens equation. The multiplicity of solutions originates from higher-order corrections in the deflection angle induced by the plasma medium [110] and the quantum-corrected spacetime geometry, rather than from strong-field photon looping effects.

The total magnification μ_Σ of all images can be expressed as the ratio of the total observed flux $I_{\rm tot}$ to the intrinsic flux of the source I_*, which in the weak-field limit takes the form Morozova et al. [111]

$$\mu_\Sigma = \frac{I_{\rm tot}}{I_*} = \sum_k \left|\left(\frac{\theta_k}{\gamma}\right)\left(\frac{d\theta_k}{d\gamma}\right)\right|, \quad k = 1, 2, \ldots, n, \tag{45}$$

where $\theta_k = x + \gamma/3$ denotes the angular position of each image.

Using these expressions, we numerically evaluate the total magnification and its dependence on both the source position and the deformation parameter β. Fig. 8 shows the variation of magnification with the angular position of the source (lower panel) and individual image magnifications (upper panel). The results reveal that:

- The total magnification decreases as the source position angle γ increases.
- A larger value of the quantum parameter β enhances the total magnification, indicating a stronger gravitational lensing effect.
- The magnification of the tertiary weak-field image remains extremely small compared to the primary and secondary images, rendering it observationally negligible.

These findings suggest that the presence of both plasma and quantum corrections can substantially modify the observable lensing signatures, thereby offering a potential avenue to test the influence of quantum-gravity corrections in astrophysical lensing systems.

4.1. Multiplicity of images and Einstein angle

In the quantum-corrected black hole spacetime, the cubic structure of Eq. (39) allows for up to three distinct images of the same source, depending on the line-of-sight angle γ and the spacetime parameters ω_0^2/ω^2 and β. As shown in Fig. 10, for sufficiently small γ and moderate values of ω_0^2/ω^2 and β, three real image solutions are obtained.

After determining the Einstein angle, we compute the Einstein radius corresponding to each image and display their configurations in Fig. 10 with the source fixed at $\gamma = 0$. In these plots, the red dashed curve denotes the primary image, the black solid curve the secondary image, and the blue dashed line the tertiary weak-field image. The green dotted circle corresponds to the Einstein ring in the standard Schwarzschild case.

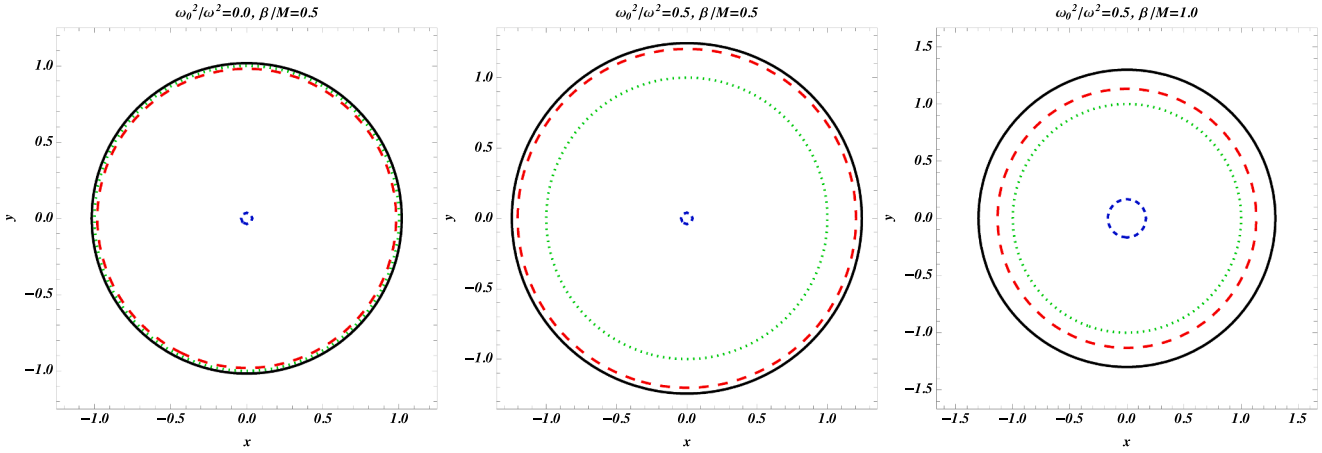

Fig. 10. Einstein ring structures for primary, secondary, and third-order relativistic images in the quantum-corrected spacetime. Left panel: $\beta/M = 0$, $\omega_0^2/\omega^2 = 0.5$; middle panel: $\beta/M = 1$, $\omega_0^2/\omega^2 = 0.5$; right panel: $\beta/M = 1$, $\omega_0^2/\omega^2 = 0.5$. Black solid curves correspond to the primary image, red dashed and blue dashed curves represent secondary and tertiary images, respectively. The green dotted line illustrates the classical GR prediction for the Einstein ring. (For interpretation of the references to colour in this figure legend, the reader is referred to the web version of this article.)

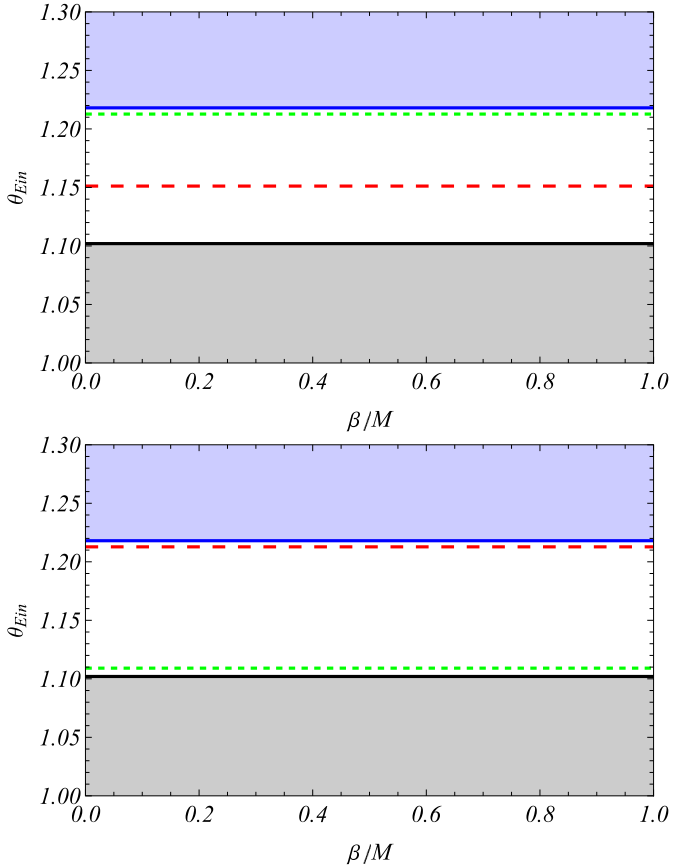

Fig. 11. Constraints on the parameters $(\omega_0^2/\omega^2, \beta/M)$ from observations of J0008–0004 (left panel) and J0029–0055 (right panel). Shaded regions correspond to excluded parameter space, while colored lines mark representative values of ω_0^2/ω^2.

Table 1
Measured quantities from selected SLACS strong lensing systems. z_l and z_s are the lens and source redshifts, respectively, θ_{Ein} denotes the Einstein ring angular radius, and the lens mass is estimated in units of $10^{10} M_\odot$.

LensID	z_s	z_l	θ_{Ein} (")	Lens Mass
J0008-0004	1.192	0.44	1.16	35 ± 4
J0029-0055	0.931	0.227	0.96	12 ± 1

Our analysis shows that for certain values of ω_0^2/ω^2 and β/M, both the primary and secondary Einstein rings appear significantly larger than in the GR limit. Physically, the parameter ω_0^2/ω^2 effectively enhances the gravitational coupling, deepening the potential well and increasing light deflection. The quantum correction parameter β/M introduces additional modifications to the effective potential, which can slightly enlarge or shift the apparent angular size of the rings, particularly affecting the third weak-field image radius.

To connect theory with observations, we utilize data from the Sloan Lens ACS (SLACS) Survey [112–114], which provides well-measured strong lensing systems with precisely determined Einstein ring radii and redshifts. Table 1 summarizes two representative lenses, J0008–0004 and J0029–0055, along with their lens and source redshifts, observed Einstein radii, and estimated lensing masses. These systems serve as testbeds to constrain the parameter space of the quantum-corrected gravity model and the plasma environment.

By fitting the theoretical predictions of our model to these observations, we numerically determine the allowed regions for $(\omega_0^2/\omega^2, \beta/M)$, illustrated in Fig. 11. For J0008–0004, the viable parameter space extends approximately from $(0, 0)$ to $(0.18, 1)$ in the absence of plasma, while for J0029–0055, the admissible range spans $(0.4, 0)$ to $(0.55, 1)$. Note that the upper bounds on β/M arise from the physical requirement of the black hole horizon's existence, preventing the emergence of a naked singularity. We emphasize that the interpretation of Einstein ring observations in realistic galaxy-scale lenses involves several astrophysical complexities that are not explicitly modeled in the present analysis. In particular, SLACS lenses are characterized by extended mass distributions, lens ellipticity, external shear from the surrounding environment, line-of-sight structures, and potential substructure within the lens galaxy. In addition, uncertainties in the plasma distribution, baryonic feedback, and deviations from spherical symmetry can further affect photon trajectories. In this work, we adopt a simplified point-mass lens approximation and an idealized plasma model in order to isolate the leading-order effects of the Kazakov–Solodukhin spacetime on Einstein ring observables. While the inclusion of realistic lens modeling and environmental effects is expected to broaden the allowed parameter space and introduce additional degeneracies, these effects primarily modify the detailed morphology and angular structure of the lensed images rather than the characteristic Einstein ring radius used in our anal-

ysis. Consequently, the constraints presented here should be regarded as indicative sensitivity bounds, demonstrating the potential of strong lensing observations to probe quantum-corrected black hole geometries under controlled assumptions.

5. Discussion and conclusion

Gravitational lensing and black hole shadow properties have been extensively investigated for a variety of modified and regular black hole spacetimes. However, the present work exhibits several key distinctions from existing studies. The Kazakov–Solodukhin (KS) black hole represents a quantum-corrected Schwarzschild geometry motivated by semiclassical considerations, rather than an ad hoc regular metric or a deformation induced by additional matter fields [115], such as nonlinear electrodynamics [6], dark photons [116], or dilatonic couplings [117]. This fundamental difference leads to qualitatively distinct observational signatures. A notable qualitative distinction emerges in the behavior of shadow and photon sphere observables. In several regular and phenomenological black hole models, including Bardeen, Hayward, and Simpson–Visser spacetimes, increasing the deformation parameter typically results in a reduction of the shadow radius. In contrast, our analysis shows that the KS quantum correction parameter β induces an enlargement of both the photon sphere and the shadow radius. This qualitatively opposite trend provides a clear observational discriminator between KS black holes and other regular or modified black hole scenarios. Furthermore, our study explicitly demonstrates that plasma effects can either enhance or suppress the sensitivity of lensing and shadow observables to the quantum correction parameter. We show that the plasma distribution introduces a nontrivial degeneracy between β and the plasma frequency, implying that plasma environments can partially mimic or mask quantum corrections to the spacetime geometry. This plasma–geometry interplay has not been systematically explored in previous studies of black hole shadows and gravitational lensing. In this work, we have investigated the weak gravitational lensing and shadow properties of KS black holes immersed in a plasma medium, focusing on how both the quantum correction parameter β/M and the plasma distribution influence observable optical signatures. Our main results can be summarized as follows:

- Increasing the quantum correction parameter β/M leads to a larger photon sphere radius and, consequently, to an enlarged black hole shadow.
- Shadow observables and lensing quantities exhibit sensitivity to both β/M and the plasma frequency, allowing indicative constraints to be inferred using observational inputs such as Event Horizon Telescope shadow measurements.
- The deflection angle of light rays displays a mild but systematic dependence on the quantum correction parameter, indicating that weak lensing observables can encode signatures of quantum-corrected spacetime geometry.
- Both uniform and inhomogeneous plasma distributions were considered. Uniform plasma enhances the deflection angle through refractive effects, whereas a singular isothermal sphere (SIS) plasma profile leads to a reduction of the deflection angle as the plasma frequency increases.
- Plasma effects significantly modify photon trajectories, particularly in the inhomogeneous SIS model, where deviations from the vacuum case become more pronounced.
- Using the lens equation in the weak-field regime, we analyzed image magnifications and Einstein ring radii, deriving indicative bounds on β/M and the plasma frequency.

While these findings highlight the potential of shadow and lensing observables as probes of KS black hole spacetimes, several limitations of the present analysis should be emphasized. Our study relies on idealized assumptions, including spherical symmetry, simplified plasma models, point-mass lens approximations, and the neglect of astrophysical systematics such as accretion flow uncertainties, lens ellipticity, external shear, and environmental effects. Consequently, the derived constraints should be interpreted as sensitivity bounds rather than definitive parameter estimates. Despite these limitations, our results provide a useful theoretical benchmark for assessing the observational distinguishability of quantum-corrected black holes. Ongoing and future observational programs-including improved Event Horizon Telescope observations, next-generation very-long-baseline interferometry arrays, and high-precision strong lensing surveys-are expected to significantly reduce observational uncertainties and may enable more stringent tests of quantum-corrected gravity models. A comprehensive analysis incorporating realistic plasma distributions, detailed lens mass modeling, and systematic uncertainties within a joint inference framework represents a natural and important direction for future work. Overall, this study underscores the importance of combining black hole shadow observations and gravitational lensing measurements as complementary tools for probing quantum modifications of black hole spacetimes in realistic astrophysical environments.

CRediT authorship contribution statement

Bekzod Rahmatov: Writing – review & editing, Writing – original draft, Supervision, Methodology; **Isomiddin Nishonov:** Software, Formal analysis; **Sardor Murodov:** Writing – review & editing, Formal analysis; **Islom Egamberdiev:** Writing – original draft, Software; **Otabek Umarov:** Writing – original draft, Methodology; **Shavkat Karshiboev:** Software, Formal analysis; **Murodbek Vapayev:** Software, Formal analysis; **Muhammad Matyoqubov:** Conceptualization.

Data availability

No data was used for the research described in the article.

Declaration of competing interest

We are drawing the editor's attention to the following facts, which may be considered as potential conflicts of interest and significant financial contributions to this work. We confirm that there are no known conflicts of interest associated with this publication, and there has been no significant financial support for this work that could have influenced its outcome. Furthermore, we confirm that the manuscript has been read and approved by all named authors and that no other persons have satisfied the criteria for authorship but are not listed. Not only that, but we further confirm that all have approved the order of authors listed in the manuscript. Furthermore, we confirm that we have given due consideration to the protection of intellectual property associated with this work and that there are no impediments to publication, including the timing of publication, for intellectual property. In so doing, we confirm that we have followed the regulations of our institutions concerning intellectual property. We further confirm that any aspect of the work covered in this manuscript that has involved either experimental animals or human patients has been conducted with the ethical approval of all relevant bodies and that such approvals are acknowledged within the manuscript. The corresponding Author is responsible for communicating with the other authors about progress, submissions of revisions, and final approval of proofs. We confirm that we have provided a current, correct email address accessible by the Corresponding Author.

Acknowledgments

B.R. and I.N. Thanks to the grant FL-7923051796 for the scientific project within the framework of Uzbek-Belarusian cooperation. S.M. gratefully acknowledges support from Grant FZ-20200929385 of the Agency of Innovative Developments of the Republic of Uzbekistan.

References

[1] S.W. Hawking, A variational principle for black holes, Commun. Math. Phys. 33 (4) (1973) 323–334. https://doi.org/10.1007/BF01646744

[2] R. Penrose, R.M. Floyd, 'Extraction of rotational energy from a black Hole', Nat. Phys. Sci. 229 (1971) 177. https://doi.org/10.1038/physci229177a0

[3] C.M. Will, The Confrontation between General Relativity and Experiment, Living Rev. Relativ. 17 (1) (2014) 4. arXiv:1403.7377 [gr-qc]. https://doi.org/10.12942/lrr-2014-4

[4] B.P. Abbott, Observation of gravitational waves from a binary black hole merger, in: C.A. Zen Vasconcellos (Ed.), Centennial of General Relativity: A Celebration, 2017, pp. 291–311. https://doi.org/10.1142/9789814699662_0011

[5] B.P. Abbott, et al., Searches for Gravitational Waves from Known Pulsars at Two Harmonics in 2015–2017 LIGO Data, Astrophys. J. 879 (1) (2019) 10. arXiv:1902.08507 [astro-ph.HE]. https://doi.org/10.3847/1538-4357/ab20cb

[6] J.M. Bardeen, W.H. Press, S.A. Teukolsky, Rotating black holes: locally nonrotating frames, energy extraction, and scalar synchrotron radiation, Astrophys. J. 178 (1972) 347–370. https://doi.org/10.1086/151796

[7] D.I. Kazakov, S.N. Solodukhin, On quantum deformation of the Schwarzschild solution, Nucl. Phys. B 429 (1) (1994) 153–176. arXiv:hep-th/9310150 [hep-th]. https://doi.org/10.1016/S0550-3213(94)80045-6

[8] S. Saghafi, K. Nozari, Shadow Behavior of the Quantum-Corrected Schwarzschild Black Hole Immersed in Holographic Quintessence, arXiv e-prints (2023) [hep-th]. https://doi.org/10.48550/arXiv.2306.13767

[9] R.A. Konoplya, Quantum corrected black holes: Quasinormal modes, scattering, shadows, Phys. Lett. B 804 (2020) 135363. arXiv:1912.10582 [gr-qc]. https://doi.org/10.1016/j.physletb.2020.135363

[10] S. Bolokhov, K. Bronnikov, R. Konoplya, Overtones' Outburst and Hawking Evaporation of Kazakov-Solodukhin Quantum Corrected Black Hole, Fortschr. Phys. 73 (5) (2025) 2400187. arXiv:2306.11083 [gr-qc]. https://doi.org/10.1002/prop.202400187

[11] K. Nozari, M. Hajebrahimi, S. Saghafi, Quantum corrections to the accretion onto a Schwarzschild black hole in the background of quintessence, Eur. Phys. J. C 80 (12) (2020) 1208. arXiv:2101.05054 [gr-qc]. https://doi.org/10.1140/epjc/s10052-020-08782-2

[12] S. Guo, Y.-X. Huang, K. Liu, E.-W. Liang, K. Lin, Influence of quantum correction on the Schwarzschild black hole polarized image, Eur. Phys. J. C 84 (6) (2024) 601. arXiv:2405.12808 [gr-qc]. https://doi.org/10.1140/epjc/s10052-024-12941-0

[13] Y.-X. Huang, S. Guo, Y.-H. Cui, Q.-Q. Jiang, K. Lin, Influence of accretion disk on the optical appearance of the Kazakov-Solodukhin black hole, Phys. Rev. D 107 (12) (2023) 123009. arXiv:2311.00302 [gr-qc]. https://doi.org/10.1103/PhysRevD.107.123009

[14] K. Nozari, M. Hajebrahimi, Geodesic Structure of the Quantum-Corrected Schwarzschild Black Hole Surrounded by Quintessence, arXiv e-prints (2020) [gr-qc]. https://doi.org/10.48550/arXiv.2004.14775

[15] M. Hajebrahimi, K. Nozari, A quantum-corrected approach to black hole radiation via a tunneling process, Progr. Theoret. Exper. Phys. 2020 (4) (2020) 043E03. arXiv:2004.14206 [gr-qc]. https://doi.org/10.1093/ptep/ptaa032

[16] I. Nishonov, B. Rahmatov, S.U. Khan, M. Zahid, J. Rayimbaev, I. Ibragimov, E. Davletov, Yukawa black holes in modified gravity: from thermodynamics to particle collisions, Ann. Phys. 486 (2026) 170332. https://doi.org/10.1016/j.aop.2025.170332

[17] A.S. Eddington, Space, Time and Gravitation. An Outline of the General Relativity Theory, 1920.

[18] F.W. Dyson, A.S. Eddington, C. Davidson, A determination of the deflection of light by the Sun's gravitational field, from observations made at the total eclipse of may 29, 1919, Phil. Trans. R. Soc. 220 (1920) 291–333. https://doi.org/10.1098/rsta.1920.0009

[19] V. Perlick, Gravitational lensing from a spacetime perspective, Living Rev. Relativ. 7 (1) (2004) 9. https://doi.org/10.12942/lrr-2004-9

[20] R.A. Vanderveld, M.J. Mortonson, W. Hu, T. Eifler, Testing dark energy paradigms with weak gravitational lensing, Phys. Rev. D 85 (10) (2012) 103518. arXiv:1203.3195 [astro-ph.CO]. https://doi.org/10.1103/PhysRevD.85.103518

[21] H.-J. He, Z. Zhang, Direct probe of dark energy through gravitational lensing effect, J. Cosmol. A. P. 2017 (8) (2017) 036. arXiv:1701.03418 [astro-ph.CO]. https://doi.org/10.1088/1475-7516/2017/08/036

[22] S. Jung, C.S. Shin, Gravitational-Wave Fringes at LIGO: Detecting Compact Dark Matter by Gravitational Lensing, Phys. Rev. Lett. 122 (4) (2019) 041103. arXiv:1712.01396 [astro-ph.CO]. https://doi.org/10.1103/PhysRevLett.122.041103

[23] C.M. Will, The 1919 measurement of the deflection of light, Class. Quant. Grav. 32 (12) (2015) 124001. arXiv:1409.7812 [physics.hist-ph]. https://doi.org/10.1088/0264-9381/32/12/124001

[24] A.O. Petters, H. Levine, J. Wambsganss, Singularity Theory and Gravitational Lensing, 2001.

[25] C.R. Keeton, A.O. Petters, Formalism for testing theories of gravity using lensing by compact objects: Static, spherically symmetric case, Phys. Rev. D 72 (10) (2005) 104006. arXiv:gr-qc/0511019 [gr-qc]. https://doi.org/10.1103/PhysRevD.72.104006

[26] M.C. Werner, A.O. Petters, Magnification relations for Kerr lensing and testing cosmic censorship, Phys. Rev. D 76 (6) (2007) 064024. arXiv:0706.0132 [gr-qc]. https://doi.org/10.1103/PhysRevD.76.064024

[27] K.S. Virbhadra, G.F.R. Ellis, 'Schwarzschild black hole lensing', Phys. Rev. D. 62 (2000) 084003. https://doi.org/10.1103/PhysRevD.62.084003

[28] M. Sereno, F. de Luca, Analytical Kerr black hole lensing in the weak deflection limit, Phys. Rev. D 74 (12) (2006) 123009. arXiv:astro-ph/0609435 [astro-ph]. https://doi.org/10.1103/PhysRevD.74.123009

[29] V. Bozza, S. Capozziello, G. Iovane, G. Scarpetta, Strong Field Limit of Black Hole Gravitational Lensing, Gen. Rel. Grav. 33 (9) (2001) 1535–1548. arXiv:gr-qc/0102068 [gr-qc]. https://doi.org/10.1023/A:1012292927358

[30] V. Bozza, Gravitational lensing in the strong field limit, Phys. Rev. D 66 (10) (2002) 103001. arXiv:gr-qc/0208075 [gr-qc]. https://doi.org/10.1103/PhysRevD.66.103001

[31] N.U. Molla, H. Chaudhary, G. Mustafa, F. Atamurotov, U. Debnath, D. Arora, Strong gravitational lensing by S g r A* and M 87* black holes embedded in dark matter halo exhibiting string cloud and quintessential field, Eur. Phys. J. C 84 (6) (2024) 574. arXiv:2310.14234 [gr-qc]. https://doi.org/10.1140/epjc/s10052-024-12917-0

[32] S.E. Vázquez, E.P. Esteban, Strong-field gravitational lensing by a Kerr black hole, Nuovo Cim. B 119 (5) (2004) 489. arXiv:gr-qc/0308023 [gr-qc]. https://doi.org/10.1393/ncb/i2004-10121-y

[33] S.U. Islam, J. Kumar, S.G. Ghosh, Strong gravitational lensing by rotating Simpson-Visser black holes, J. Cosmol. A. P. 2021 (10) (2021) 013. arXiv:2104.00696 [gr-qc]. https://doi.org/10.1088/1475-7516/2021/10/013

[34] J. Kumar, S.U. Islam, S.G. Ghosh, Investigating strong gravitational lensing effects by supermassive black holes with Horndeski gravity, Eur. Phys. J. C 82 (5) (2022) 443. arXiv:2109.04450 [gr-qc]. https://doi.org/10.1140/epjc/s10052-022-10357-2

[35] N.U. Molla, S.G. Ghosh, U. Debnath, Testing gravitational lensing effects by supermassive massive black holes with superstring theory metric: astrophysical implications and EHT constraints, Phys. Dark Univ. 44 (2024) 101495. https://doi.org/10.1016/j.dark.2024.101495

[36] S.-S. Zhao, Y. Xie, Strong deflection lensing by a Lee-Wick black hole, Phys. Lett. B 774 (2017) 357–361. https://doi.org/10.1016/j.physletb.2017.09.090

[37] M. Sereno, Gravitational lensing by stars with angular momentum, Mon. Not. Roy. Astron. Soc. 344 (3) (2003) 942–950. arXiv:astro-ph/0307243 [astro-ph]. https://doi.org/10.1046/j.1365-8711.2003.06881.x

[38] S. Saydullayev, I. Nishonov, M. Dusaliyev, O. Xoldorov, S. Murodov, S. Karshiboev, S. Urinov, B. Rahmatov, Black hole surrounded by perfect fluid dark matter in STV gravity: particle dynamics, thermodynamics, gravitational weak lensing and EHT tests, Eur. Phys. J. C 85 (9) (2025) 1081. https://doi.org/10.1140/epjc/s10052-025-14780-z

[39] A.S. Majumdar, N. Mukherjee, Gravitational Lensing in the Weak Field Limit by a Braneworld Black Hole, Mod. Phys. Lett. A 20 (32) (2005) 2487–2496. arXiv:astro-ph/0403405 [astro-ph]. https://doi.org/10.1142/S0217732305017676

[40] A. Övgün, K. Jusufi, İ. Sakallı, Gravitational lensing under the effect of Weyl and bumblebee gravities: applications of gauss-Bonnet theorem, Ann. Phys. (N.Y.) 399 (2018) 193–203. https://doi.org/10.1016/j.aop.2018.10.012

[41] R.C. Pantig, E.T. Rodulfo, Weak deflection angle of a dirty black hole, Chin. J. Phys. 66 (2020) 691–702. arXiv:2003.00764 [gr-qc]. https://doi.org/10.1016/j.cjph.2020.06.015

[42] G. Mustafa, F. Atamurotov, I. Hussain, S. Shaymatov, A. Övgün, Shadows and gravitational weak lensing by the Schwarzschild black hole in the string cloud background with quintessential field, Chin. Phys. C 46 (12) (2022) 125107. arXiv:2207.07608 [gr-qc]. https://doi.org/10.1088/1674-1137/ac917f

[43] H. Liu, J. Liang, J. Jia, Deflection and gravitational lensing of null and timelike signals in the Kiselev black hole spacetime in the weak field limit, Class. Quant. Grav. 39 (19) (2022) 195013. arXiv:2204.04519 [gr-qc]. https://doi.org/10.1088/1361-6382/ac8b56

[44] A. Övgün, Weak field deflection angle by regular black holes with cosmic strings using the Gauss-Bonnet theorem, Phys. Rev. D 99 (10) (2019) 104075. arXiv:1902.04411 [gr-qc]. https://doi.org/10.1103/PhysRevD.99.104075

[45] W. Javed, M.B. Khadim, J. Abbas, A. Övgün, Weak gravitational lensing by stringy black holes, Eur. Phys. J. Plus 135 (3) (2020) 314. arXiv:2004.00408 [gr-qc]. https://doi.org/10.1140/epjp/s13360-020-00322-x

[46] C.-Y. Wang, Y.-F. Shen, Y. Xie, Weak and strong deflection gravitational lensings by a charged Horndeski black hole, J. Cosmol. A. P. 2019 (4) (2019) 022. arXiv:1902.03789 [gr-qc]. https://doi.org/10.1088/1475-7516/2019/04/022

[47] G.N. Gyulchev, S.S. Yazadjiev, Analytical Kerr-Sen Dilaton-Axion Black Hole Lensing in the Weak Deflection Limit, Phys. Rev. D 81 (2010) 023005. arXiv:0909.3014 [gr-qc]. https://doi.org/10.1103/PhysRevD.81.023005

[48] K. Jusufi, A. Övgün, J. Saavedra, Y. Vásquez, P.A. González, Deflection of light by rotating regular black holes using the Gauss-Bonnet theorem, Phys. Rev. D 97 (12) (2018) 124024. arXiv:1804.00643 [gr-qc]. https://doi.org/10.1103/PhysRevD.97.124024

[49] N. Parbin, D.J. Gogoi, U.D. Goswami, Weak gravitational lensing and shadow cast by rotating black holes in axionic Chern-Simons theory, Phys. Dark Univ. 41 (2023) 101265. arXiv:2305.09157 [gr-qc]. https://doi.org/10.1016/j.dark.2023.101265

[50] V. Perlick, Ray Optics, Fermat's Principle, and Applications to General Relativity, 61, 2000.

[51] O.Y. Tsupko, G.S. Bisnovatyi-Kogan, Relativistic rings due to Schwarzschild gravitational lensing, Gravit. Cosmol. 15 (2) (2009) 184–187. https://doi.org/10.1134/S0202289309020182

[52] G.S. Bisnovatyi-Kogan, O.Y. Tsupko, 'Gravitational lensing in a non-uniform plasma', Mon. Not. R. Astron. Soc. 404 (2010) 1790. https://doi.org/10.1111/j.1365-2966.2010.16290.x

[53] A. Rogers, Frequency-dependent effects of gravitational lensing within plasma, Mon. Not. Roy. Astron. Soc. 451 (1) (2015) 17–25. arXiv:1505.06790 [gr-qc]. https://doi.org/10.1093/mnras/stv903

[54] X. Er, A. Rogers, Two families of astrophysical diverging lens models, Mon. Not. R. Astron. Soc. 475 (1) (2018) 867–878. arXiv:1712.06900 [astro-ph.GA]. https://doi.org/10.1093/mnras/stx3290
[55] F. Atamurotov, S. Shaymatov, P. Sheoran, S. Siwach, Charged black hole in 4D Einstein-Gauss-Bonnet gravity: particle motion, plasma effect on weak gravitational lensing and centre-of-mass energy, J. Cosmol. A. P. 2021 (8) (2021) 045. arXiv:2105.02214 [gr-qc]. https://doi.org/10.1088/1475-7516/2021/08/045
[56] G.Z. Babar, F. Atamurotov, A.Z. Babar, Gravitational lensing in 4-D Einstein-Gauss-Bonnet gravity in the presence of plasma, Phys. Dark Univ. 32 (2021) 100798. https://doi.org/10.1016/j.dark.2021.100798
[57] G.Z. Babar, F. Atamurotov, S. Ul Islam, S.G. Ghosh, Particle acceleration around rotating Einstein-Born-Infeld black hole and plasma effect on gravitational lensing, Phys, Rev. D 103 (8) (2021) 084057. arXiv:2104.00714 [gr-qc]. https://doi.org/10.1103/PhysRevD.103.084057
[58] A. Hakimov, F. Atamurotov, 'Gravitational lensing by a non-Schwarzschild black hole in a plasma', Astrophys. Space. Sci. 361 (2016) 112. https://doi.org/10.1007/s10509-016-2702-7
[59] F. Atamurotov, A. Abdujabbarov, J. Rayimbaev, Weak gravitational lensing Schwarzschild-MOG black hole in plasma, Eur. Phys. J. C 81 (2) (2021) 118. https://doi.org/10.1140/epjc/s10052-021-08919-x
[60] B. Rahmatov, M. Zahid, S.U. Khan, J. Rayimbaev, I. Ibragimov, Z. Yuldoshev, A. Dauletov, S. Muminov, Black holes in general relativity coupled with nonlinear electrodynamics surrounded by perfect fluid dark matter: thermodynamics, particle motion, and black hole shadow, Chin. Phys. C 49 (7) (2025) 075105. https://doi.org/10.1088/1674-1137/adc188
[61] C.A. Benavides-Gallego, A.A. Abdujabbarov, Bambi, 'Gravitational lensing for a boosted Kerr black hole in the presence of plasma', Eur. Phys. J. C. 78 (2018) 694. https://doi.org/10.1140/epjc/s10052-018-6170-97
[62] O.Y. Tsupko, Deflection of light rays by a spherically symmetric black hole in a dispersive medium, Phys. Rev. D 103 (10) (2021) 104019. arXiv:2102.00553 [gr-qc]. https://doi.org/10.1103/PhysRevD.103.104019
[63] W. Javed, I. Hussain, A. Övgün, Weak deflection angle of Kazakov-Solodukhin black hole in plasma medium using Gauss-Bonnet theorem and its greybody bonding, Eur. Phys. J. Plus 137 (1) (2022) 148. arXiv:2201.09879 [gr-qc]. https://doi.org/10.1140/epjp/s13360-022-02374-7
[64] G. Crisnejo, E. Gallo, Weak lensing in a plasma medium and gravitational deflection of massive particles using the Gauss-Bonnet theorem. A unified treatment, Phys. Rev. D 97 (12) (2018) 124016. arXiv:1804.05473 [gr-qc]. https://doi.org/10.1103/PhysRevD.97.124016
[65] H. Chakrabarty, A.B. Abdikamalov, A.A. Abdujabbarov, C. Bambi, Weak gravitational lensing: a compact object with arbitrary quadrupole moment immersed in plasma, Phys. Rev. D. 98 (2018) 024022. https://doi.org/10.1103/PhysRevD.98.024022
[66] B. Rahmatov, I. Egamberdiev, O. Umarov, M. Vapayev, S. Karshiboev, Y. Turaev, S. Murodov, Astrophysical signatures of rotating Kazakov-Solodukhin black holes: shadows and constraints from EHT observations, Nucl. Phys. B 1022 (2026) 117212. https://doi.org/10.1016/j.nuclphysb.2025.117212
[67] H. Hoshimov, O. Yunusov, F. Atamurotov, M. Jamil, A. Abdujabbarov, Weak gravitational lensing and shadow of a GUP-modified Schwarzschild black hole in the presence of plasma, Phys. Dark Univ. 43 (2024) 101392. arXiv:2312.10678 [gr-qc]. https://doi.org/10.1016/j.dark.2023.101392
[68] F. Atamurotov, O. Yunusov, A. Abdujabbarov, G. Mustafa, Gravitational weak lensing of hairy black hole in presence of plasma, New Astron. 105 (2024) 102098. https://doi.org/10.1016/j.newast.2023.102098
[69] F. Atamurotov, H. Alibekov, A. Abdujabbarov, G. Mustafa, M.M. Aripov, Weak gravitational lensing around Bardeen black hole with a string cloud in the presence of plasma, Symmet. (Basel) 15 (4) (2023) 848. https://doi.org/10.3390/sym15040848
[70] F. Atamurotov, I. Hussain, G. Mustafa, A. Övgün, Weak deflection angle and shadow cast by the charged-Kiselev black hole with cloud of strings in plasma, Chin. Phys. C 47 (2) (2023) 025102. https://doi.org/10.1088/1674-1137/ac9fbb
[71] F. Atamurotov, S.G. Ghosh, Gravitational weak lensing by a naked singularity in plasma, Eur. Phys. J. Plus 137 (6) (2022) 662. https://doi.org/10.1140/epjp/s13360-022-02885-3
[72] F. Atamurotov, F. Sarikulov, V. Khamidov, A. Abdujabbarov, Gravitational weak lensing of Schwarzschild-like black hole in presence of plasma, Eur. Phys. J. Plus 137 (2022) 567. https://doi.org/10.1140/epjp/s13360-022-02780-x
[73] V. Perlick, O.Y. Tsupko, Light propagation in a plasma on Kerr spacetime: Separation of the Hamilton-Jacobi equation and calculation of the shadow, Phys. Rev. D. 95 (10) (2017) 104003. arXiv:1702.08768 [gr-qc]. https://doi.org/10.1103/PhysRevD.95.104003
[74] J. Badía, E.F. Eiroa, Shadow of axisymmetric, stationary, and asymptotically flat black holes in the presence of plasma, Phys. Rev. D 104 (8) (2021) 084055. arXiv:2106.07601 [gr-qc]. https://doi.org/10.1103/PhysRevD.104.084055
[75] F. Atamurotov, B. Ahmedov, A. Abdujabbarov, Optical properties of black holes in the presence of a plasma: The shadow, Phys. Rev. D 92 (8) (2015) 084005. arXiv:1507.08131 [gr-qc]. https://doi.org/10.1103/PhysRevD.92.084005
[76] Q. Li, Y. Zhu, T. Wang, Gravitational effect of plasma particles on the shadow of Schwarzschild black holes, Eur. Phys. J. C 82 (1) (2022) 2. arXiv:2102.00957 [gr-qc]. https://doi.org/10.1140/epjc/s10052-021-09959-z
[77] A. Chowdhuri, A. Bhattacharyya, Shadow analysis for rotating black holes in the presence of plasma for an expanding universe, Phys. Rev. D 104 (6) (2021) 064039. arXiv:2012.12914 [gr-qc]. https://doi.org/10.1103/PhysRevD.104.064039
[78] Y. Pahlavon, F. Atamurotov, K. Jusufi, M. Jamil, A. Abdujabbarov, Effect of magnetized plasma on shadow and gravitational lensing of a Reissner–Nordström black hole, Phys. Dark Univ. 45 (2024) 101543. arXiv:2406.09431 [gr-qc]. https://doi.org/10.1016/j.dark.2024.101543
[79] F. Atamurotov, M. Jamil, K. Jusufi, Quantum effects on the black hole shadow and deflection angle in the presence of plasma, Chin. Phys. C 47 (3) (2023) 035106. arXiv:2212.12949 [gr-qc]. https://doi.org/10.1088/1674-1137/acaef7
[80] F. Atamurotov, I. Hussain, G. Mustafa, K. Jusufi, Shadow and quasinormal modes of the Kerr-Newman-Kiselev-Letelier black hole, Eur. Phys. J. C 82 (9) (2022) 831. arXiv:2209.01652 [gr-qc]. https://doi.org/10.1140/epjc/s10052-022-10782-3
[81] F. Tello-Ortiz, M. Ali Raza, M. Zubair, Y. Gómez-Leyton, No Cauchy horizon in a gravitational decoupled Reissner–Nordström spacetime, Phys. Dark Univ. 44 (2024) 101460. https://doi.org/10.1016/j.dark.2024.101460
[82] M. Zubair, M.A. Raza, F. Sarikulov, J. Rayimbaev, 4D Einstein-Gauss-Bonnet black hole in Power-Yang-Mills field: a shadow study, JCAP 10 (2023) 058. arXiv:2305.16888 [gr-qc]. https://doi.org/10.1088/1475-7516/2023/10/058
[83] B. Rahmatov, I. Egamberdiev, S. Murodov, J. Rayimbaev, I. Ibragimov, E. Davletov, S. Djumanov, Gravitational lensing by black holes surrounded by PFDM in Kalb-Ramond gravity in plasma medium, Phys. Dark Univ. 50 (2025) 102152. https://doi.org/10.1016/j.dark.2025.102152
[84] O. Yunusov, F. Atamurotov, I. Hussain, A. Abdujabbarov, G. Mustafa, Energetic processes and thermodynamic analysis of the spinning Kiselev black hole with cloud of strings, Chin. J. Phys. 90 (2024) 608–623. https://doi.org/10.1016/j.cjph.2024.06.006
[85] O. Yunusov, B. Turimov, Y. Khamroev, S. Usanov, F. Turaev, M. Kuliyeva, Charged Zipoy–Voorhees metric in string theory, Ann. Phys. 481 (2025) 170151. https://doi.org/10.1016/j.aop.2025.170151
[86] O. Yunusov, J. Rayimbaev, F. Sarikulov, M. Zahid, A. Abdujabbarov, Z. Stuchlík, Rotating charged black holes in EMS theory: shadow studies and constraints from EHT observations, Eur. Phys. J. C 84 (12) (2024) 1240. https://doi.org/10.1140/epjc/s10052-024-13500-3
[87] M. Zahid, O. Yunusov, C. Shen, J. Rayimbaev, S. Muminov, Shadows and quasinormal modes of rotating black holes in Horndeski theory: parameter constraints using EHT observations of M87* and Sgr A*, Phys. Dark Univ. 47 (2025) 101734. https://doi.org/10.1016/j.dark.2024.101734
[88] K.E. Akiyama, et al., First M87 Event Horizon Telescope Results. I. The Shadow of the Supermassive Black Hole, Astrophys. J. 875 (1) (2019) L1. arXiv:1906.11238 [astro-ph.GA]. https://doi.org/10.3847/2041-8213/ab0ec7
[89] K.E. Akiyama, et al., First Sagittarius A* event horizon telescope results. I. The shadow of the supermassive black hole in the center of the Milky Way, Astrophys. J. 930 (2) (2022) L12. https://doi.org/10.3847/2041-8213/ac6674
[90] L. Meliyeva, O. Xoldorov, O. Tursunboyev, S. Karshiboev, S. Murodov, I. Nishonov, B. Rahmatov, Theoretical study of strong gravitational lensing around dyonic Mod-Max black hole: constraints from EHT observations, Chin. Phys. 49 (12) (2025) 125102. https://doi.org/10.1088/1674-1137/adf4a0
[91] B. Rahmatov, S. Murodov, J. Rayimbaev, S. Muminov, I. Ibragimov, R. Eshburiev, QPO Tests and charged particles around regular Ayón-Beato-Garcia black holes, Phys. Dark Univ. 50 (2025) 102102. https://doi.org/10.1016/j.dark.2025.102102
[92] K.E. Akiyama, et al., First Sagittarius A* event horizon telescope results. III. Imaging of the galactic center supermassive black hole, Astrophys. J. 930 (2) (2022) L14. https://doi.org/10.3847/2041-8213/ac6429
[93] B. Rahmatov, M. Zahid, J. Rayimbaev, R. Rahim, S. Murodov, QPOs and circular orbits around black holes in Chaplygin-like cold dark matter, Chin. J. Phys. 92 (2024) 143–165. https://doi.org/10.1016/j.cjph.2024.09.002
[94] K. Akiyama, et al. The persistent shadow of the supermassive black hole of M 87. I. observations, calibration, imaging, and analysis, Astron. Astrophys. 681 (2024) A79. https://doi.org/10.1051/0004-6361/202347932
[95] J.L. Synge (Ed.), Relativity: The General theory, 1960.
[96] V. Perlick, O.Y. Tsupko, G.S. Bisnovatyi-Kogan, Influence of a plasma on the shadow of a spherically symmetric black hole, Phys. Rev. D 92 (10) (2015) 104031. arXiv:1507.04217 [gr-qc]. https://doi.org/10.1103/PhysRevD.92.104031
[97] O.Y. Tsupko, G.S. Bisnovatyi-Kogan, 'Gravitational lensing in plasmic medium', Plasma Phys. Rep. 41 (2015) 562. https://doi.org/10.1134/S1063780X15070016
[98] O.Y. Tsupko, G.S. Bisnovatyi-Kogan, Gravitational lensing in the presence of plasmas and strong gravitational fields, Gravit. Cosmol. 20 (3) (2014) 220–225. https://doi.org/10.1134/S0202289314030153
[99] G.S. Bisnovatyi-Kogan, O.Y. Tsupko, Shadow of a black hole at cosmological distances, Universe 3 (2017) 57. https://doi.org/10.3390/universe3030057. https://doi.org/10.3390/universe3030057
[100] V. Perlick, 'Gravitational lensing from a spacetime perspective', Living Rev. Relativ. 7 (2004) 9. https://doi.org/10.12942/lrr-2004-9
[101] G.S. Bisnovatyi-Kogan, O.Y. Tsupko, Gravitational lensing in a non-uniform plasma, Mon. Not. Roy. Astron. Soc. 404 (2010) 1790–1800. arXiv:1006.2321 [astro-ph.CO]. https://doi.org/10.1111/j.1365-2966.2010.16290.x
[102] F. Atamurotov, K. Jusufi, M. Jamil, A. Abdujabbarov, M. Azreg-Aïnou, Axion-plasmon or magnetized plasma effect on an observable shadow and gravitational lensing of a Schwarzschild black hole, Phys. Rev. D 104 (6) (2021) 064053. arXiv:2109.08150 [gr-qc]. https://doi.org/10.1103/PhysRevD.104.064053
[103] M.A. Raza, M. Zubair, E. Maqsood, Influence of plasma on the optical appearance of spinning black hole in Kalb-Ramond gravity and its existence around M87* and Sgr A*, JCAP 05 (2024) 047. arXiv:2401.04779 [gr-qc]. https://doi.org/10.1088/1475-7516/2024/05/047
[104] M.A. Raza, J. Rayimbaev, F. Sarikulov, M. Zubair, B. Ahmedov, Z. Stuchlik, Shadow of novel rotating black hole in GR coupled to nonlinear electrodynamics and constraints from EHT results, Phys. Dark Univ. 44 (2024) 101488. arXiv:2311.15784 [gr-qc]. https://doi.org/10.1016/j.dark.2024.101488
[105] K. Akiyama, et al., Event Horizon Telescope, First M87 event horizon telescope results. VIII. Magnetic field structure near the event horizon, Astrophys. J. Lett.

910 (1) (2021) L13. arXiv:2105.01173 [astro-ph.HE]. https://doi.org/10.3847/2041-8213/abe4de

[106] K. Akiyama, et al., Event Horizon Telescope, First Sagittarius A* event horizon telescope results. I. The shadow of the supermassive black hole in the center of the Milky Way, Astrophys. J. Lett. 930 (2) (2022) L12. arXiv:2311.08680 [astro-ph.HE]. https://doi.org/10.3847/2041-8213/ac6674

[107] S. Vagnozzi, R. Roy, Y.-D. Tsai, L. Visinelli, M. Afrin, A. Allahyari, P. Bambhaniya, D. Dey, S.G. Ghosh, P.S. Joshi, K. Jusufi, M. Khodadi, R.K. Walia, A. Övgün, C. Bambi, Horizon-scale tests of gravity theories and fundamental physics from the event horizon telescope image of Sagittarius A (*), Class. Quant. Grav. 40 (16) (2023) 165007. arXiv:2205.07787 [gr-qc]. https://doi.org/10.1088/1361-6382/acd97b

[108] B. BEZDĚKOVÁ, Electromagnetic Waves in Dispersiveand Refractive Relativistic Systems, Master's thesis, Diplomová práce, vedoucí Bičák, Jiří. Praha: Univerzita Karlova, Matematicko-fyzikálnífakulta,Ústav teoretické fyziky„ 2019.

[109] D. Umarov, O. Yunusov, F. Atamurotov, A. Abdujabbarov, S.G. Ghosh, Plasma effects on weak gravitational lensing and shadows of Sen black holes, Chin. Phys. C 49 (5) (2025) 055102. https://doi.org/10.1088/1674-1137/adb384

[110] B. Turimov, B. Ahmedov, A. Abdujabbarov, C. Bambi, Gravitational lensing by a magnetized compact object in the presence of plasma, Int. J. Mod. Phys. D 28 (16) (2019) 2040013. arXiv:1802.03293 [gr-qc]. https://doi.org/10.1142/S0218271820400131

[111] V.S. Morozova, B.J. Ahmedov, A.A. Tursunov, Gravitational lensing by a rotating massive object in a plasma, Astrophys. Space. Sci. 346 (2) (2013) 513–520. https://doi.org/10.1007/s10509-013-1458-6

[112] R. Gavazzi, T. Treu, L.V.E. Koopmans, A.S. Bolton, L.A. Moustakas, S. Burles, P.J. Marshall, The Sloan Lens ACS Survey. VI. Discovery and Analysis of a Double Einstein Ring, Astrophys. J. 677 (2) (2008) 1046–1059. arXiv:0801.1555 [astro-ph]. https://doi.org/10.1086/529541

[113] A.S. Bolton, S. Burles, L.V.E. Koopmans, T. Treu, L.A. Moustakas, The Sloan Lens ACS Survey. I. A Large Spectroscopically Selected Sample of Massive Early-Type Lens Galaxies, Astrophys. J. 638 (2) (2006) 703–724. arXiv:astro-ph/0511453 [astro-ph]. https://doi.org/10.1086/498884

[114] Z. Horváth, L.Á. Gergely, Z. Keresztes, T. Harko, F.S.N. Lobo, Constraining Hořava-Lifshitz gravity by weak and strong gravitational lensing, Phys. Rev. D 84 (8) (2011) 083006. arXiv:1105.0765 [gr-qc]. https://doi.org/10.1103/PhysRevD.84.083006

[115] S. Chaudhary, Shadows and intensities of Simpson–Visser black holes in Verlinde's emergent gravity, Commun. Theor. Phys. 77 (12) (2025). https://doi.org/10.1088/1572-9494/addfc5

[116] S. Chaudhary, M.D. Sultan, T. Anwar, A.M.A. EI-Rehim, F. Atamurotov, A.M. Mubaraki, M. Hadi, M.A. Sayed, Gravitational lensing, shadow images and accretion dynamics of dark photon corrected black holes, Ann. Phys. (N.Y.) 485 (2026) 170302. https://doi.org/10.1016/j.aop.2025.170302

[117] S. Chaudhary, T. Anwar, F. Atamurotov, A.M. Mubaraki, M.M. Alam, Gravitational lensing and shadows of dilatonic black holes in dilaton-massive gravity, Nucl. Phys. B 1018 (2025) 117075. https://doi.org/10.1016/j.nuclphysb.2025.117075